Fractional forest cover mapping in the Brazilian Amazon with a combination of MODIS and TM images

Dengsheng Lu [a] , Mateus Batistella [b] , Emilio Moran [a] , Scott
Hetrick [a] , Diogenes Alves [c] & Eduardo Brondizio [a]

[a] Anthropological Center for Training and Research on Global
Environmental Change (ACT), Indiana University, Bloomington, IN,
47405, USA

[b] Brazilian Agricultural Research Corporation, EMBRAPA Satellite
Monitoring, Campinas, São Paulo, Brazil

[c] Instituto Nacional de Pesquisas Espaciais (INPE), Divisao de
Processamento de Imagens (DPI), Sao Jose dos Campos, Brazil

Available online: 01 Aug 2011

First

PLEASE SCROLL DOWN FOR ARTICLE

Taylor & Francis
Taylor & Francis Group

Fractional forest cover mapping in the Brazilian Amazon with a combination of MODIS and TM images

DENGSHENG LU∗†, MATEUS BATISTELLA‡, EMILIO MORAN†, SCOTT
HETRICK†, DIOGENES ALVES§ and EDUARDO BRONDIZIO†

†Anthropological Center for Training and Research on Global Environmental Change
(ACT), Indiana University, Bloomington, IN 47405, USA
‡Brazilian Agricultural Research Corporation, EMBRAPA Satellite Monitoring,
Campinas, São Paulo, Brazil
§Instituto Nacional de Pesquisas Espaciais (INPE), Divisao de Processamento de
Imagens (DPI), Sao Jose dos Campos, Brazil

High deforestation rates in Amazonia have motivated considerable efforts to monitor forest changes with satellite images, but mapping forest distribution and monitoring change at a regional scale remain a challenge. This article proposes a new approach based on the integrated use of Moderate Resolution Imaging Spectroradiometer (MODIS) and Landsat Thematic Mapper (TM) images to rapidly map forest distribution in Rondônia, Brazil. The TM images are used to differentiate forest and non-forest areas and the MODIS images are used to extract three fraction images (vegetation, shade and soil) with linear spectral mixture analysis (LSMA). A regression model is built to calibrate the MODIS-derived forest results. This approach is applied to the MODIS image in 2004 and is then transferred to other MODIS images. Compared to INPE PRODES (Brazil's Instituto Nacional de Pesquisas Espaciais – Programme for the Estimation of Deforestation in the Brazilian Amazon) data, the errors for total forest area estimates in 2000, 2004 and 2006 are −0.97%, 0.81% and −1.92%, respectively. This research provides a promising approach for mapping fractional forest (proportion of forest cover area in a pixel) distribution at a regional scale. The major advantage is that this procedure can rapidly provide the spatial and temporal patterns of fractional forest cover distribution at a regional scale by the integrated use of MODIS images and a limited number of Landsat images.

1. Introduction

The increasing world population and associated urbanization and environmental degradation have resulted in a continuous decrease in the world's forest area, especially primary forest (FAO 2006, 2007). Providing timely forest resource information at regional and global scales is important for addressing biodiversity, climate change, desertification and environmental problems (FAO 2006). Deforestation has been recognized as an important contributor to carbon emissions, climate change and loss of biodiversity (Skole *et al*. 1994, Fearnside 1996, 2005, Tian *et al*. 1998,

*Corresponding author. Email: dlu@indiana.edu

Hirsch *et al.* 2004). The Brazilian Amazon basin contains the largest continuous rainforest in the world. Its vast areas of tropical forest represent a potentially large source of carbon/greenhouse gases emissions if deforested. Since the 1970s, deforestation in this region has increased from 152 000 km^2 in 1978 to 718 550 km^2 in 2007 (Alves 2007, INPE 2008). To monitor the deforestation rate, Brazil's Instituto Nacional de Pesquisas Espaciais (INPE) has developed two systems: the Programme for the Estimation of Deforestation in the Brazilian Amazon (PRODES; www.obt.inpe.br/prodes/) and the Real Time Deforestation Monitoring System (DETER; www.obt.inpe.br/deter/). PRODES uses Landsat Thematic Mapper (TM) images mostly acquired during the dry season (May–September for regions south of the equator, November–March for northern parts of the basin) for detection of newly deforested areas and estimation of annual deforestation rates in the Legal Amazon (The Legal Amazon is the largest socio-geographic division of the South American nation of Brazil, containing all of its territory in the Amazon Basin, encompassing all seven states of the north region (Acre, Amapá, Amazonas, Pará, Rondônia, Roraima and Tocantins), the centre-west region of Mato Grosso state and the northeast region of Maranhão state) and requires a few months of work to complete an entire survey (Hansen *et al.* 2008b). Cloud cover in the Amazon often makes it difficult to obtain cloud-free TM images (Asner 2001). DETER uses Moderate Resolution Imaging Spectroradiometer (MODIS) data to identify new clearing hotspots in areas greater than 25 ha, but does not produce estimates of deforestation.

Remotely sensed data have become a primary data source for mapping land use/cover distribution and monitoring its changes at different scales (Franklin and Wulder 2002). Many approaches have been developed for land-cover classification (Lu and Weng 2007) but most of them are based on the spectral features of remotely sensed data, where each pixel is classified into one class, even using coarse spatial resolution data from, for example, the National Oceanic and Atmospheric Administration (NOAA) Advanced Very High Resolution Radiometer (AVHRR), Satellite Pour l'Observation de la Terre (SPOT) VEGETATION and MODIS (DeFries and Townshend 1994, DeFries *et al.* 1998, Hansen *et al.* 2000, Friedl *et al.* 2002, Latifovic *et al.* 2004, Giri *et al.* 2005, Lowry *et al.* 2007). Landsat images are probably the most common data source used for land use/cover classification (Adams *et al.* 1995, Roberts *et al.* 2002, Vieira *et al.* 2003, Lu *et al.* 2004, 2008) because of their suitable spectral and spatial resolutions (Franklin and Wulder 2002). However, for regional or global land-cover assessments, the relatively small-scene footprint of medium spatial resolution images such as Landsat TM require huge volumes of data, making their use difficult due to prohibitive amounts of processing time and labour. An additional difficulty is data acquisition in conditions of low revisit time because of cloud cover over large areas, especially in the moist tropical regions. Hence, coarse spatial resolution images such as AVHRR, SPOT VEGETATION and MODIS are often used for regional or global land-cover mapping (Latifovic *et al.* 2004, Wessels *et al.* 2004, Giri *et al.* 2005).

Different approaches have been used for land-cover mapping using coarse spatial resolution images at regional and global scales (e.g. Sedano *et al.* 2005, Carreiras *et al.* 2006a). Although pixel-based classification approaches are frequently used for regional or global land-cover mapping, land-cover estimations show large uncertainties (Wang and Tenhunen 2004, Waser and Schwarz 2006, Sivanpillai *et al.* 2007) because of the mixed pixel problem. In traditional per-pixel classifications, selection of training samples for image classifications and selection of test samples for

accuracy assessment are often very difficult with coarse spatial resolution images (McIver and Friedl 2001). An alternative solution is to develop approaches to estimate the fraction of land cover within each pixel by linking coarse spatial resolution with medium spatial resolution images (Hansen and DeFries 2004, Latifovic and Olthof 2004). Considerable efforts have been made to reduce the mixed pixel problem and many techniques have been explored (Shimabukuro and Smith 1991, 1995, Iverson *et al*. 1994, Zhu and Evans 1994, Mayaux and Lambin 1995, DeFries *et al*. 1997, 2000, Foody *et al*. 1997, Hagen *et al*. 2002, Hansen *et al*. 2002a,b, 2003, Braswell *et al*. 2003, Hansen and DeFries 2004, Haertel and Shimabukuro 2005, Schwarz and Zimmermann 2005, Carreiras *et al*. 2006b, Olthof and Fraser 2007, Tottrup *et al*. 2007), including regression trees, regression models and linear spectral mixture algorithms.

Previous research has been mainly site specific, and therefore transferability of the developed models to different data sets for estimation of fractional land cover has not been examined. The main reason is that the previous approaches are based on the use of spectral responses which are often influenced by the variation of biophysical environments. The objectives of the current research were to test a new approach to timely and accurately map fractional forest area (i.e. the proportion of primary forest accounted for in a pixel) at a regional scale with the integration of coarse and medium spatial resolution images in the moist tropical region in the Brazilian Amazon, and to explore the model transferability among different image datasets in Rondônia, Brazil. The proposed method can rapidly update forest change data sets with limited time and labour, in comparison with the PRODES, which requires intensive labour and time in developing forest data using Landsat TM data and has difficulty in collecting cloud-free images, and DETER, which only detects hotspots with deforestation areas greater than 25 ha. Another advantage of the proposed method lies in its model transfer in improving forest area estimation accuracy without the use of Landsat images after the calibration model is established.

2. Method

Rondônia is located in the northwest region of the Brazil Amazon and was selected as the study area in this research (figure 1). Rondônia ranks third in the largest deforestation percentages over time in the Brazilian Amazon (the first two largest deforestation states are Mato Grosso and Pará) (INPE 2008). To improve area estimation accuracy and the spatial patterns of forest distribution, the development of new approaches for mapping fractional forest cover distribution is necessary. Figure 2 illustrates the framework for estimating fractional forest cover at a regional scale. Fractional forest cover means the proportion of primary forest accounted for in a pixel (e.g. in a MODIS pixel). The major steps include (1) development of green vegetation, shade and soil fraction images with linear spectral mixture analysis (LSMA) of the MODIS multispectral image; (2) extraction of an initial vegetation class using a thresholding approach based on the fraction images; (3) extraction of MODIS spectral signatures based on the initial vegetation class and MODIS surface reflectance images; (4) refinement of the initial vegetation class to produce a pixel-based forest image; (5) extraction of an initial fractional forest image by combining the soil fraction and the pixel-based forest image; (6) development of a calibration model for calibrating the initial fractional forest image based on the selected samples from the overlapped areas between MODIS-derived initial fractional forest image and the Landsat TM-derived fractional
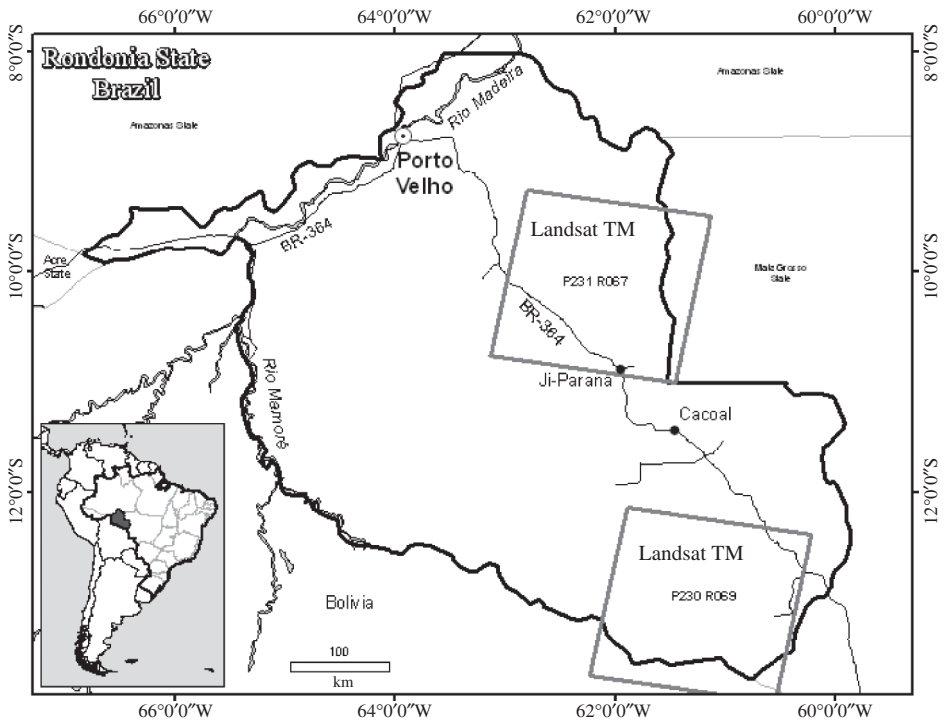
Figure 1.   Study area: Rondônia state and location of the two Landsat TM images selected.

forest image; and (7) evaluation of the final fractional forest images by using new samples from the Landsat TM-derived forest images. The total forest area was also compared with the PRODES data sets. Finally, the developed calibration model was transferred to other MODIS data sets for estimating fractional forest areas.

2.1   *Data preparation*

MODIS 8-day surface reflectance (MOD09A1) images for 2000, 2004 and 2006 were initially inspected and the images presenting the least clouds were selected for this research (table 1). The 8-day MODIS composites were downloaded from the U.S. Geological Survey (USGS) Global Visualization Viewer (http://glovis.usgs.gov/). All MODIS images were reprojected into Albers Conical Equal Area. The selected MODIS images (three tiles: h11v09, h11v10 and h12v10) were mosaicked to form a complete image for the state of Rondônia. The original 463 m MODIS 8-day composites were resampled to 450 m resolution using the nearest-neighbour algorithm.

The Landsat TM images were obtained from INPE Brazil. All TM images were reprojected to the Albers Conical Equal Area and the nearest-neighbour technique was used to resample TM images to a pixel size of 30 × 30 m during the image reprojection. The registration errors for all TM images were less than 0.5 pixel. These images were atmospherically calibrated into surface reflectance with the dark object subtraction method (Lu *et al*. 2002). The TM images were overlapped on the MODIS colour composite for a visual examination of the geometric accuracy based on a comparison
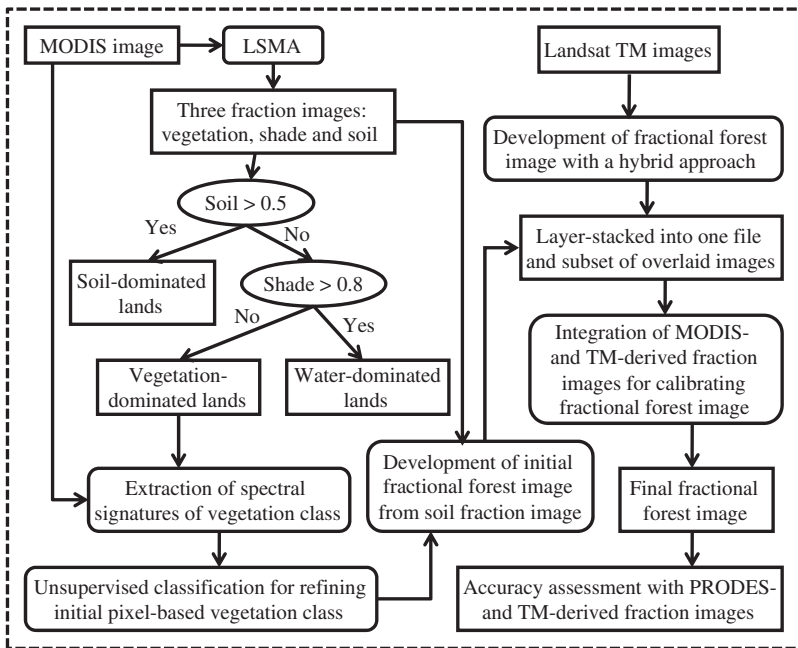
Figure 2. Framework of mapping fractional forest-cover distribution at the regional scale based on a combination of Terra MODIS and Landsat TM images.

Table 1. Data sets used in the current research.

Image acquisition dates for Terra MODIS	Image acquisition dates for Landsat TM (path/row)	The year for PRODES product
24–31 August 2000	15 July 2000 (231/67) 9 August 2000 (230/69)	2000
28 August–4 September 2004	26 July 2004 (231/67) 4 August 2004 (230/69)	2004
12–19 July 2006	No TM images	2006

of the geometric accuracy between the linear features, such as rivers, and the boundaries between different land covers. We found that the geometric accuracy was very good and met our research purposes for the forest mapping and monitoring with the MODIS data.

In this research, INPE PRODES data products with geographic information system (GIS) shapefile format in 2000, 2004 and 2006 were collected and used to evaluate the total forest area estimates which were developed from MODIS data sets. In this product, forest distribution was mapped from Landsat TM images (www.obt.inpe.br/prodes/) based on the image segmentation of the soil and shade fraction images from the LSMA, followed by unsupervised classification and image editing (Shimabukuro *et al*. 1998, Hansen *et al*. 2008b).

2.2 *Mapping forest cover distribution from Landsat images*

Tropical forests can be grouped roughly into categories of primary forest and successional forests. Primary forest is defined here as a forest that is not greatly disturbed by natural disasters or human activities. Successional forest is defined here as a regrowth forest following a disturbance such as deforestation. To map forest distribution, a hybrid approach consisting of thresholding and an unsupervised algorithm based on Landsat TM images was used, as illustrated in figure 3. The Landsat normalized difference vegetation index (NDVI) images, which were calculated for each Landsat TM image based on red and near-infrared bands (i.e. (NIR – Red)/(NIR + Red)), were used to produce an initial forest image using a thresholding technique. The thresholds were identified based on 15–20 sample plots of primary forest for each scene of an TM NDVI image, respectively. The statistics (mean, standard deviation, minimum and maximum) of the sample plots were calculated. The thresholds were then selected according to the ranges of mean $\pm$ 2.5 SD and adjusted by checking the minimum and maximum values, so that all pixels with forest were extracted, but as many as possible of the non-forest pixels were excluded. The thresholds were selected separately based on each NDVI image. Because some advanced successional forests have similar NDVI values to those of primary forest, they are difficult to be separated automatically from the NDVI thresholds. We used an unsupervised algorithm to refine the initial forest image based on our previous research in this study area (Lu *et al.* 2003, 2004, 2008). The spectral signatures of the TM bands for the initial forest class were extracted based on the following rules: if the pixel belongs to initial forest class, the spectral signature is extracted from the TM bands, otherwise a zero value is assigned to the pixel. The Iterative Self-Organizing Data Analysis Technique (ISODATA) algorithm was then used to classify the extracted spectral signatures of the initial forest class into 50 clusters and the analyst was responsible for assigning the resulting clusters to forest or non-forest.

Accuracy assessment for each TM-derived forest image was conducted based on randomly selected sample plots. We have previously carried out research related to land use/cover classification with Landsat TM images and field surveys and have had experience in separating forest from other land covers in this study area (Lu *et al.* 2003, 2004, 2008). To evaluate the forest classification image, 200 sample plots were randomly selected for each forest image and each sample plot was examined with visual interpretation of the corresponding TM colour composite based on our previous research. The TM-derived forest images with 30 m spatial resolution were aggregated with the mean algorithm to generate fractional forest images with a spatial resolution of 450 m, the same spatial resolution as the MODIS data used in the study area. These developed forest images were used as reference data for evaluating MODIS-derived fractional forest cover images and for developing a calibration model to calibrate the MODIS-derived results, based on separately selected samples from the overlapped areas between TM- and MODIS-derived forest images.

2.3 *Mapping fractional forest cover distribution from MODIS data*

2.3.1 LSMA. LSMA is regarded as a physically based image processing tool that supports repeatable and accurate extraction of quantitative subpixel information (Smith *et al.* 1990, Adams *et al.* 1995, Mustard and Sunshine 1999). To produce high-quality fraction images, a key step is to select suitable endmembers. Many methods have been developed to identify endmembers (Lu *et al.* 2003, Theseira *et al.* 2003)
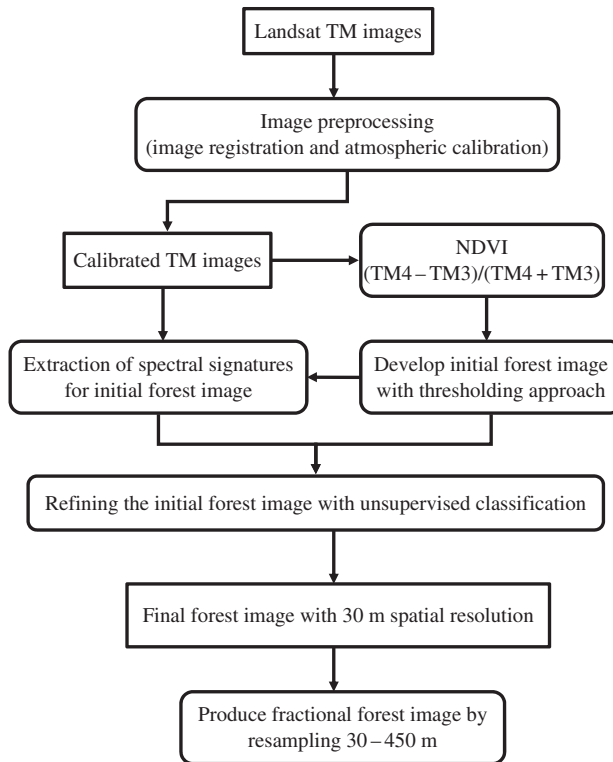
Figure 3. Strategy of mapping forest distribution at the local scale from Landsat TM images with a hybrid approach. TM4 and TM3 represent the spectral bands 4 (near-infrared) and 3 (red wavelength) in Landsat TM imagery.

and image-based endmember selection approaches are often used. Previous studies have shown that the use of a minimum noise fraction (MNF) transform can improve the quality of fraction images (Cochrane and Souza 1998, van der Meer and de Jong 2000). In this research, the MNF procedure was applied to transform the six MODIS spectral bands into a new coordinate set, of which the first three MNF components accounted for the majority of the information (approximately 99%) in the MODIS data. During endmember selection, it is important to consider the spatial scale of the data sets used and to avoid outliers when endmembers are determined from the image itself (Lu *et al*. 2003, 2004). In this research, three endmembers (vegetation, shade and soil) were selected from the MNF components with the assistance of the Landsat TM images. The shade endmember is usually difficult to identify from the MODIS image, but clear and deep water can be used as a proxy (Shimabukuro and Smith 1995). By linking MODIS colour composite and corresponding TM images, the vegetation endmember was initially selected from the areas of dense secondary forests and the soil endmember was initially selected from bare soils in agricultural lands. These initial endmembers were compared with those endmembers selected from the scatterplot of the first and second MNF components and the scatterplot of the first and third MNF components. The endmembers whose curves were similar but located at the extreme vertices of the scatterplot were finally selected. In this way, the impact of cloud or

shadow contamination on the MODIS images was avoided. After selection of the end-members, a constrained least-squares solution was applied to unmix the six MODIS spectral bands (MODIS band 5 was not used due to the striping problem) into fraction images. The same procedure was used separately to develop fraction images from each MODIS image.

2.3.2   Extraction of pixel-based forest images from MODIS images.   Three major land covers (a soil-dominated class, a water-dominated class and a vegetation-dominated class) were first classified using thresholds based on soil and shade fraction images, as shown in figure 2. A comparative analysis between Landsat TM images and the MODIS-derived fraction images indicated that urban areas, pasture and some initial successional vegetation in the dry season had high values in the soil fraction images, and water or wetland with less vegetation cover had high values in the shade fraction image. After these non-forest land covers with high values in the soil and shade fraction images were masked out with a thresholding technique, the remaining pixels were the vegetation-dominated class, including primary forest and advanced successional forest. To further refine the vegetation-dominated class, MODIS surface reflectance for the vegetation-dominated class was extracted and the ISODATA algorithm was used to classify the extracted MODIS reflectance image into 60 clusters. The analyst was then responsible for assigning the clusters into forest and non-forest classes with the assistance of the Landsat TM images.

2.3.3   Extraction of the initial fraction forest image from the soil fraction image.
Previous research has indicated that vegetation and shade fractions are good parameters reflecting forest stand structures (Sabol *et al*. 2002, Lu *et al*. 2003). However, the vegetation and shade fractions are more sensitive to seasonal variation than the soil fraction (Lu *et al*. 2003). By contrast, the soil fraction has proven to be reliable for detecting forest changes in the Amazon (Anderson *et al*. 2005). From the view of remote sensing spectral signatures, the components of forested lands can be assumed to be composed of green vegetation, canopy shade, non-photosynthetic vegetation (NPV; i.e. branches and stems) and soil. For dense forest lands, the soil fraction is close to zero. Forest may be mixed with other land covers when the forested land is less than 25 ha. This is especially true in the boundaries between forest and other land covers and the forest remnants. To improve the forest estimation accuracy and the spatial pattern of forest distribution, excluding the non-forest proportion in the mixed pixels is necessary. When only three endmembers are used, the proportion of forest area in a pixel includes green vegetation and canopy-cast shadow. The sum of vegetation, shade and soil fractions should be unity if the error is ignored. Considering the reliability of the soil fraction in multitemporal MODIS images, the fractional forest cover area in a pixel is thus defined as:

$$f_{\text{forest}} = 1 - f_{\text{soil}} \tag{1}$$

where f_{forest} and f_{soil} are the proportion of forest and soil cover in a pixel, respectively, and their values are between 0 and 1. As the pixel-based forest image had already been developed using the combination of the thresholding technique and unsupervised classification, the linkage of the pixel-based forest image and the f_{forest} image was

used to produce the fractional forest image by excluding the non-forest pixels with the following rule: if the pixel belongs to the forest class in the pixel-based forest image, the pixel value is extracted from the f_{forest} image, otherwise a value of zero is assigned to the pixel. This hybrid approach based on LSMA, thresholding and unsupervised classification for mapping fractional forest cover distribution was first examined in the 2004 MODIS image, and then applied to f_{forest} and 2006 MODIS data.

2.4 *Development of a calibration model and its application at a regional scale*

Evaluation of the MODIS-derived fraction forest image with the Landsat-derived fractional forest images indicated that a systematic underestimation occurred for the pixels with a relatively small proportion of forest area in a pixel. Therefore, developing a calibration model for modifying the MODIS-based fractional forest images was necessary. A calibration model was first developed with the regression analysis based on the 2004 TM- and MODIS-derived fractional forest images. The TM- and MODIS-derived fractional forest images were stacked into one file and the overlapping areas were then cut out for further analysis. Pixel samples were selected on the overlapped TM- and MODIS-derived fraction images at every five pixels, considering the size of sample population and the correlation between neighbouring pixels. The selected samples were used to develop a regression model in which the TM-derived fraction image was used as the dependent variable and the MODIS-derived fraction image as the independent variable. Analysis of the scatterplot between the two variables from the TM- and MODIS-derived fractional forest images indicated a linear relationship between these two variables. Thus, a linear regression model was developed and then used to calibrate the MODIS-derived fraction images. The correlation coefficients between the reference data and the MODIS estimates were also calculated to further evaluate the quality of model fit. The developed model based on the 2004 TM and MODIS data was transferred to other MODIS-derived fractional forest images respectively, to calibrate the fractional forest areas and to examine the feasibility of model transferability.

2.5 *Accuracy assessment*

Accuracy assessment is important in evaluating model performance and the reliability of the results. The overall accuracy, kappa coefficient, and the producer's and user's accuracy are often used to evaluate the land-cover classification accuracy (Congalton 1991, Foody 2002). However, they are valid only for pixel-based classification images. In this research we used the root mean square error (RMSE) and system error (SE) to evaluate the MODIS-derived fractional forest images. In general, lower values of the RSME and SE indicate higher accuracy of the results. Use of SE also indicates whether the results are underestimated or overestimated within error ranges.

Three levels of window sizes (one pixel, nine pixels (3×3) and 25 pixels (5×5)) were selected to examine how the estimation errors changed as selected window sizes varied. The samples were independently selected from the overlapping areas between the selected TM- and MODIS-images. The stacked file including TM and MODIS overlapped areas with 450 m spatial resolution was further aggregated into 1350 m (i.e. 3×3 window size) and 2250 m (i.e. 5×5 window size) with a mean algorithm. The sampling intervals of 10, 5 and 3 on the MODIS-derived images with a spatial resolution of 450, 1350 and 2250 m, respectively, were used to select sample plots for the accuracy assessment.

In addition to the accuracy assessment based on samples, the total forest area developed from the MODIS data sets was compared with the INPE PRODES data set, which was developed from Landsat TM images (Hansen *et al*. 2008b, INPE 2008). Because the PRODES data set is only available in a GIS shapefile (vector format) with geographic projection, it cannot be used directly for comparison with MODIS-derived results (raster format) at the pixel level. Therefore, the total forest areas from the PRODES products for 2000, 2004 and 2006 were calculated and compared to the corresponding MODIS-derived total forest areas. The overall error of forest area (OEF) for each year was calculated with following equation:

$$OEF = \frac{(E_{\text{MODIS}} - E_{\text{PRODES}})}{E_{\text{PRODES}}} \times 100 \qquad (2)$$

where E_{MODIS} and E_{PRODES} are the total forest areas estimated from the MODIS-derived fractional forest image and the reference forest area calculated from the PRODES product.

3. Results

3.1 *Evaluation of Landsat-derived forest images*

Accurate extraction of forest areas from the Landsat TM images was required because the extracted forest images were used as reference data for developing the models for calibrating the MODIS-derived results. According to the accuracy assessment results, an overall accuracy of more than 97% for each Landsat-derived forest image was achieved. In this research, the developed per-pixel based forest images with 30 m spatial resolution were aggregated to 450 m spatial resolution to produce the fractional forest images. These fractional forest images were then used for developing a calibration model and for conducting the accuracy assessment of the MODIS-derived forest products separately with independently selected samples.

3.2 *Accuracy assessment of the MODIS-derived products*

The accuracy assessment indicated that, before calibration, the forest areas derived from the MODIS data were underestimated and had high errors. Table 2 summarizes the errors with three levels of window sizes based on two Landsat-derived fractional forest images for both 2000 and 2004. The percentages of RMSE and SE are 26.6% and −11.1% at the single pixel level, and 15.6% and −9.4% for 5 × 5 window sizes, respectively. As the window size increased, RMSE and SE were reduced, and the correlation coefficient between the reference and estimate increased. This implies that the MODIS-derived fractional forest estimates may have high errors for single pixels, but these errors would be gradually decreased in a large area; thus MODIS data are suitable for mapping forest distribution in a large area.

Examining the scatterplots between the samples from the MODIS- and TM-derived fraction images confirmed the underestimation as shown in table 2. Figure 4 provides an example of the scatterplot between the MODIS- and TM-derived forest samples in 2004, indicating that a very good linear relationship existed between the TM- and MODIS-derived fractions, and the underestimation was prevalent when the proportion of forest cover in a pixel was relatively small. The linear relationship illustrated in figure 4 indicates that a linear regression model can be developed to improve the

Table 2. Accuracy assessment of MODIS-derived fractional forest cover (before calibration) for two Landsat TM-derived fractional forest images (path/row 231/67 and 230/69) for both 2000 and 2004.

	TM231/67				TM230/69			
Window size	No. of samples	SE (%)	RM (%)	*R*	No. of samples	SE (%)	RM (%)	*R*
MODIS 2004								
1 × 1	1235	−8.29	25.32	0.85	1152	−11.07	26.58	0.84
3 × 3	1326	−6.89	15.31	0.95	976	−10.48	18.64	0.93
5 × 5	1458	−6.60	12.29	0.97	1463	−9.40	15.59	0.95
MODIS 2000								
1 × 1	1280	−10.70	30.12	0.81	1270	−8.58	30.09	0.78
3 × 3	1772	−8.86	17.81	0.93	1542	−7.23	18.02	0.92
5 × 5	1442	−7.90	14.77	0.95	1301	−6.89	15.98	0.94

Note: SE, System error; RM, root mean square error; *R*, correlation coefficient.
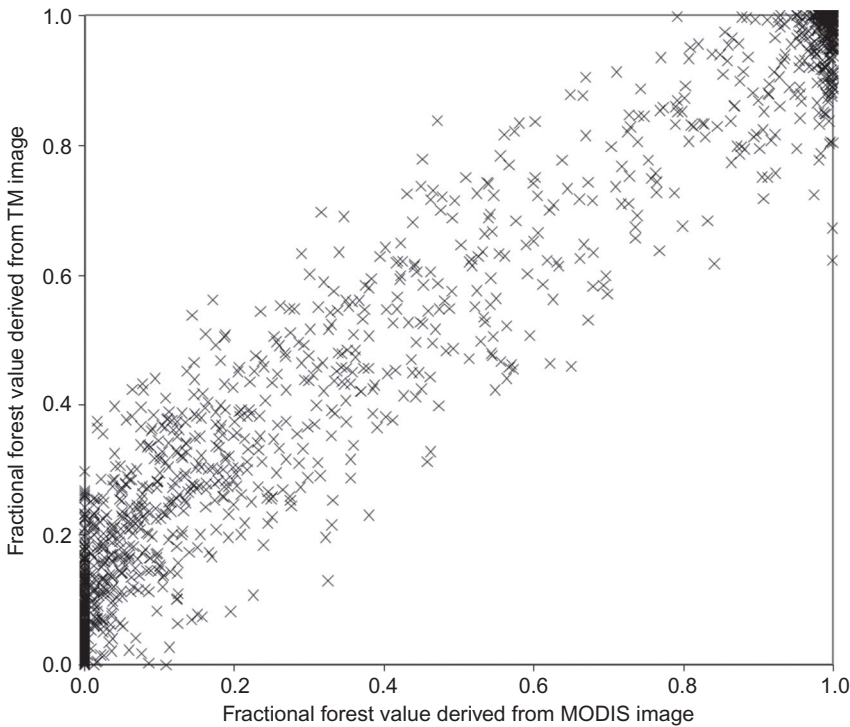

Figure 4. Scatterplot illustrating the relationship between fractional forest values from the 2004 MODIS imagery and from the corresponding Landsat TM images before calibration (window size of 5 × 5).

estimation of MODIS-derived fractional forest areas. A regression model based on the samples collected in the 2004 TM- and MODIS-derived fraction forest images is expressed as follows:

$$y = 0.8611x + 0.1262 \quad \text{when } x > 0 \tag{3}$$

$$\text{otherwise, } y = 0 \quad \text{when } x = 0 \tag{4}$$

where y is the calibrated fractional forest value and x is the MODIS-derived fractional forest value. The R^2 value for this regression model is 0.945. This model was first applied to calibrate the fractional forest area from the 2004 MODIS-derived image, and then transferred to the 2000 and 2006 MODIS-derived products. After calibration, the SE and RMSE at the per-pixel level were, respectively, 1.56% and 4.19% in 2004, and 2.37% and 5.58% in 2000. The accuracy assessment also indicated that errors after calibration were reduced, implying that calibration is necessary for improving the MODIS-derived fraction images.

An alternative accuracy assessment involved comparing the total forest areas between the MODIS-derived forest images and INPE PRODES product. The forest areas for 2000, 2004 and 2006 were calculated based on the PRODES shapefile images and the corresponding MODIS-derived forest images. The evaluation results are summarized in table 3, which shows that the total forest areas derived from the MODIS images in 2000, 2004 and 2006 are very close to the INPE PRODES results, with an accuracy as high as 98%. These results indicate that MODIS data can be successfully used for forest mapping at a regional scale.

3.3 *Spatial patterns of fractional forest distribution at a regional scale*

The fractional forest image improved the information on the spatial patterns of forest distribution compared with the per-pixel based forest images, and improved the area estimation accuracy, in particular for the areas with mixed pixels. Figure 5 shows the fractional forest distribution with (*a*) black-and-white and (*b*) false colour images for (*i*) 2000, (*ii*) 2004 and (*iii*) 2006. To more clearly demonstrate the spatial patterns of fractional forest distribution, the fractional forest image is grouped into six levels (≥ 0.9, 0.7–0.9, 0.5–0.7, 0.3–0.5, <0.3 and non-forest) and displayed in different colours. A comparison of the MODIS-derived fractional forest images and the selected Landsat TM colour composites shows that the forests located in undisturbed regions had fractional values ≥ 0.9. The values between 0.7 and 0.9 were mainly riverine forests or forests on relatively steep slopes. The values <0.7 were mainly forest remnants in the

Table 3. Comparison of forest areas for the selected years after calibration.

	Forest area (km^2)		
	2000	2004	2006
Fractional forest value in a pixel			
≥ 0.9	94 851.00	88 781.06	80 159.63
0.7–0.9	25 725.07	19 039.86	19 736.04
0.5–0.7	13 006.95	12 715.01	11 549.12
0.3–0.5	9213.83	9588.72	9291.60
<0.3	6239.52	7261.16	7251.96
Total area (km^2)	149 036.40	137 385.80	127 988.30
Reference data (km^2)	150 496.00	136 281.00	130 488.35
Overall error (%)	−0.97	0.81	−1.92

(*a*)   (*b*)
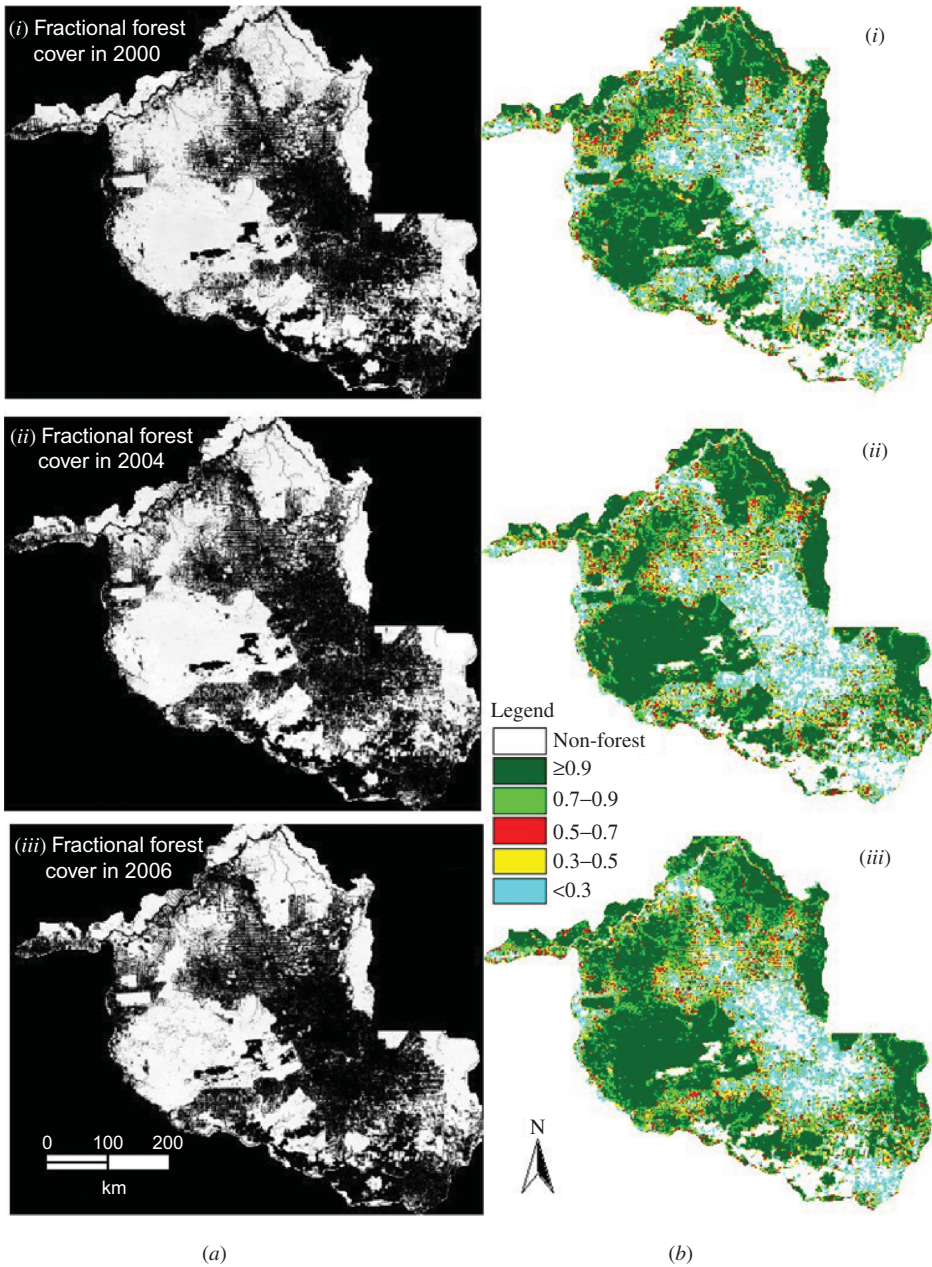
Figure 5. The estimated fractional forest cover images from (*a*) MODIS surface reflectance images in (*i*) 2000, (*ii*) 2004 and (*ii*) 2006 and (*b*) the corresponding sliced false colour images in Rondônia. The black-and-white images show forest cover distribution with white as the high proportion of forest cover in a pixel and black as no or a very small proportion of forest cover in a pixel. To better express the spatial patterns of forest distribution, the fraction value (proportion of forest cover in a pixel) was grouped into five levels and assigned a colour corresponding to each level.

deforested regions. As shown in table 3, the deforestation in Rondônia was obvious. The total forest area decreased from 149 036 km^2 in 2000 to 137 386 km^2 in 2004, and to 127 988 km^2 in 2006. During the 6 years, 21 048 km^2 forested areas were deforested according to the MODIS-derived results, comparing with 20 008 km^2 according to the INPE PRODES product for the same time period.

4.   Discussion

This research indicates that the combination of MODIS images and a limited number of TM images can be successfully used to map forest distribution and monitor forest change at a regional scale. This approach can rapidly update the spatial database of forest distribution with limited time and labour. Without calibration with the TM-derived results, the MODIS-based forest estimates underestimated the forest areas, especially when the forest cover accounted for a relatively small proportion in a pixel. In the coarse spatial resolution image, when forest is mixed with other land cover, especially soil-dominated lands such as pastures and agricultural lands in the dry season, other land-cover information may be highlighted in the spectral signatures, and thus the soil fraction may be overestimated in the LSMA approach. NPV (e.g. stems and branches) has a similar spectral signature to that of soil (Roberts *et al*. 1998). When NPV is not used in the LSMA, the soil fraction is often overestimated, and thus forest fraction in a pixel is underestimated. Therefore, calibration is necessary to mitigate this underestimation. The scatterplot between the MODIS-derived fraction forest values and the reference data indicated that there is an SE, resulting in underestimation of the fractional forest areas. The linear relationship indicated that it is possible to develop a regression model to calibrate the MODIS-derived fraction images. The improved results after calibration have confirmed that use of the combined MODIS and TM images is feasible to rapidly map forest distribution at a regional scale.

One objective of developing models is to apply them to large areas or to different data sets. Many factors can affect the model transferability, such as the explanatory variables used, the samples collected, and the effects of the biophysical environment on the explanatory variables. Previous research on fractional forest estimation was mainly directed at specific sites or data sets (DeFries *et al*. 2000, Hansen *et al*. 2002a,b, Tottrup *et al*. 2007). To our knowledge, no research has explored the transferability of the established models to different data sets. The major problem is that the variables used in these models are dependent on the spectral responses, such as the MODIS surface reflectance and vegetation indices (Iverson *et al*. 1994, DeFries *et al*. 1997, Haertel and Shimabukuro 2005, Olthof and Fraser 2007, Tottrup *et al*. 2007), which are influenced by the differences in biophysical environments. This research used the soil fraction image to infer the fractional forest areas and has shown its reliability because the soil fraction was relatively insensitive to the effects of different biophysical environments when comparing green vegetation and shade fraction images, spectral responses and vegetation indices for the forested lands (Lu *et al*. 2003). Examination of model transferability in different data sets in this research has proven that the same model can be used successfully for calibrating MODIS-based estimation results. This approach can reduce considerably the time and labour in mapping forest distribution and monitoring its change at a regional scale with coarse spatial resolution images.

With regard to regional and global land-cover classifications, MODIS data have become a major data source. The per-pixel based classification method is still common for land-cover classification on coarse spatial resolution images (Friedl *et al*.

2002, Latifovic *et al*. 2004, Wessels *et al*. 2004, Giri *et al*. 2005, Lowry *et al*. 2007, Hansen *et al*. 2008b, Potapov *et al*. 2008). However, large uncertainty often exists due to the mixed pixel problem in the coarse spatial resolution images (Wang and Tenhunen 2004, Waser and Schwarz 2006, Sivanpillai *et al*. 2007, Hansen *et al*. 2008b). Therefore, different methods such as LSMA, neural networks and regression tree models have been used to reduce the mixed pixel problem (DeFries *et al*. 2000, Foody *et al*. 1997, Hagen *et al*. 2002, Carreiras *et al*. 2006b, Tottrup *et al*. 2007). In particular, MODIS images have been used to map vegetation continuous fields (VCFs) with the regression tree algorithm (Hansen *et al*. 2002a,b, 2003), and then the VCF product is further used for other applications such as forest mapping and monitoring by combining Landsat images (Hansen *et al*. 2008a). MODIS data are valuable for coarse land-cover classification such as forest and non-forest separation (Wessels *et al*. 2004, Tottrup *et al*. 2007), but difficult for detailed land-cover classification. To improve land-cover classification performance, a combination of MODIS and Landsat images is often adopted (Hansen *et al*. 2008a, Potapov *et al*. 2008). This research has proven the importance of reducing the mixed pixel problem by the use of LSMA and the necessity of calibrating the MODIS-derived results by the established regression model based on the combination of MODIS- and TM-derived results.

5. Conclusions

Fractional forest cover mapping at a regional scale using coarse spatial resolution remotely sensed data is a challenge because of the mixed pixel problem. Pixel-based classification approaches for regional forest cover mapping from coarse spatial resolution data can generate large uncertainties. The current research proposes a new approach to mapping fractional forest areas based on the combined use of medium and coarse spatial resolution images and indicates that a combination of Landsat images and MODIS data can be successfully used to map fractional forest areas at a regional scale. The developed model can be transferred to different data sets for calibrating MODIS-derived fractional forest images. This approach can improve the spatial pattern of fractional forest distribution compared to the pixel-based approach, and can rapidly extract forest cover information with limited time and labour, compared with the use of medium spatial resolution images in a large area such as those used in INPE PRODES. This is especially valuable for timely and accurately monitoring forest change in a large area, such as the Amazon region.

References
ADAMS, J.B., SABOL, D.E., KAPOS, V., FILHO, R.A., ROBERTS, D.A., SMITH, M.O. and GILLESPIE, A.R., 1995, Classification of multispectral images based on fractions of endmembers: application to land-cover change in the Brazilian Amazon. *Remote Sensing of Environment*, **52**, pp. 137–154.

ALVES, D.S., 2007, Science and technology and sustainable development in the Brazilian Amazon. In *The Stability of Tropical Rainforest Margins: Linking Ecological, Economic and Social Constraints of Land Use and Conservation*, T. Tscharntke, C. Leuschner, M. Zeller, E. Guhardja and A. Bidin (Eds.), pp. 493–512 (Berlin: Springer-Verlag).

ANDERSON, L., SHIMABUKURO, Y.E., DEFRIES, R.S. and MORTON, D., 2005, Assessment of deforestation in near real time over the Brazilian Amazon using multitemporal fraction images derived from Terra MODIS. *IEEE Geoscience and Remote Sensing Letters*, **2**, pp. 315–318.

ASNER, G.P., 2001, Cloud cover in Landsat observations of the Brazilian Amazon. *International Journal of Remote Sensing*, **22**, pp. 3855–3862.

BRASWELL, B.H., HAGEN, S.C., FROLKING, S. and SALAS, W.A., 2003, A multivariable approach for mapping subpixel land cover distributions using MISR and MOIDS: application in the Brazilian Amazon region. *Remote Sensing of Environment*, **87**, pp. 243–256.

CARREIRAS, J.M.B., PEREIRA, J.M.C., CAMPAGNOLO, M.L. and SHIMABUKURO, Y.E., 2006a, Assessing the extent of agriculture/pasture and secondary succession forest in the Brazilian Legal Amazon using SPOT VEGETATION data. *Remote Sensing of Environment*, **101**, pp. 283–298.

CARREIRAS, J.M.B., PEREIRA, J.M.C. and SHIMABUKURO, Y.E., 2006b, Land cover mapping in the Brazilian Amazon using SPOT-4 VEGETATION data and machine learning classification methods. *Photogrammetric Engineering and Remote Sensing*, **72**, pp. 897–910.

COCHRANE, M.A. and SOUZA, C.M., JR., 1998, Linear mixture model classification of burned forests in the eastern Amazon. *International Journal of Remote Sensing*, **19**, pp. 3433–3440.

CONGALTON, R.G., 1991, A review of assessing the accuracy of classification of remotely sensed data. *Remote Sensing of Environment*, **37**, pp. 35–46.

DEFRIES, R.S., HANSEN, M., STEININGER, M., DUBAYAH, R., SOHLBERG, R. and TOWNSHEND, J., 1997, Subpixel forest cover in central Africa from multisensor, multitemporal data. *Remote Sensing of Environment*, **60**, pp. 228–246.

DEFRIES, R., HANSEN, M. and TOWNSHEND, J., 2000, Global continuous fields of vegetation characteristics: a linear mixture model applied to multiyear 8 km AVHRR data. *International Journal of Remote Sensing*, **21**, pp. 1389–1414.

DEFRIES, R.S., HANSEN, M., TOWNSHEND, J.R.G. and SOHLBERG, R., 1998, Global land cover classifications at 8 km spatial resolution: the use of training data derived from Landsat imagery in decision tree classifiers. *International Journal of Remote Sensing*, **19**, pp. 3141–3168.

DEFRIES, R.S. and TOWNSHEND, J.R.G., 1994, NDVI-derived land cover classification at global scales. *International Journal of Remote Sensing*, **15**, pp. 3567–3586.

FAO, 2006, *Global Forest Resources Assessment 2005: Progress Towards Sustainable Forest Management*. Forest Resources Assessment (FRA) Report. FAO Forestry Paper 147 (Rome: Food and Agriculture Organization).

FAO, 2007, *State of the World's Forest 2007* (Rome: Food and Agriculture Organization).

FEARNSIDE, P.M., 1996, Amazonian deforestation and global warming: carbon stocks in vegetation replacing Brazil's Amazon forest. *Forest Ecology and Management*, **80**, pp. 21–34.

FEARNSIDE, P.M., 2005, Deforestation in Brazilian Amazonia: history, rates, and consequences. *Conservation Biology*, **19**, pp. 680–688.

FOODY, G.M., 2002, Status of land cover classification accuracy assessment. *Remote Sensing of Environment*, **80**, pp. 185–201.

FOODY, G.M., LUCAS, R.M., CURRAN, P.J. and HONZAK, M., 1997, Mapping tropical forest fractional cover from coarse spatial resolution remote sensing imagery. *Plant Ecology*, **131**, pp. 143–154.

FRANKLIN, S.E. and WULDER, M.A., 2002, Remote sensing methods in medium spatial resolution satellite data land cover classification of large areas. *Progress in Physical Geography*, **26**, pp. 173–205.

FRIEDL, M.A., McIVER, D.K., HODGES, J.C.F., ZHANG, X.Y., MUCHONEY, D., STRAHLER, A.H., WOODCOCK, C.E., GOPAL, S., SCHNEIDER, A., COOPER, A., BACCINI, A., GAO, F. and SCHAAF, C., 2002, Global land cover mapping from MODIS: algorithms and early results. *Remote Sensing of Environment*, **83**, pp. 287–302.

GIRI, C., ZHU, Z. and REED, B., 2005, A comparative analysis of the global land cover 2000 and MODIS land cover data sets. *Remote Sensing of Environment*, **94**, pp. 123–132.

HAERTEL, V.F. and SHIMABUKURO, Y.E., 2005, Spectral linear mixing model in low spatial resolution image data. *IEEE Transactions on Geoscience and Remote Sensing*, **43**, pp. 2555–2562.

HAGEN, S.C., BRASWELL, B.H., FROLKING, S., SALAS, W.A. and XIAO, X., 2002, Determination of subpixel fractions of nonforested area in the Amazon using multiresolution satellite sensor data. *Journal of Geophysical Research*, **107**, 8049, doi:10.1029/2000JD000255.

HANSEN, M.C. and DeFRIES, R.S., 2004, Detecting long-term global forest change using continuous fields of tree-cover maps from 8-km advanced very high resolution radiometer (AVHRR) data for the years 1982-99. *Ecosystems*, **7**, pp. 695–716.

HANSEN, M.C., DeFRIES, R.S., TOWNSHEND, J.R.G., CARROLL, M., DIMICELI, C. and SOHLBERG, R.A., 2003, Global percent tree cover at a spatial resolution of 500 meters: first results of the MODIS vegetation continuous fields algorithm. *Earth Interactions*, **7**, pp. 1–15.

HANSEN, M.C., DeFRIES, R.S., TOWNSHEND, J.R.G., MARUFU, L. and SOHLBERG, R., 2002a, Development of a MODIS tree cover validation data set for Western Province, Zambia. *Remote Sensing of Environment*, **83**, pp. 320–335.

HANSEN, M.C., DeFRIES, R.S., TOWNSHEND, J.R.G. and SOHLBERG, R., 2000, Global land cover classification at 1 km spatial resolution using a classification tree approach. *International Journal of Remote Sensing*, **21**, pp. 1331–1364.

HANSEN, M.C., DeFRIES, R.S., TOWNSHEND, J.R.G., SOHLBERG, R., DIMICELI, C. and CARROLL, M., 2002b, Towards an operational MODIS continuous field of percent tree cover algorithm: examples using AVHRR and MODIS data. *Remote Sensing of Environment*, **83**, pp. 303–319.

HANSEN, M.C., ROY, D.P., LINDQUIST, E., ADUSEI, B., JUSTICE, C.O. and ALTSTATT, A., 2008a, A method for integrating MODIS and Landsat data for systematic monitoring of forest cover and change in the Congo Basin. *Remote Sensing of Environment*, **112**, pp. 2495–2513.

HANSEN, M.C., SHIMABUKURO, Y.E., POTAPOV, P. and PITTMAN, K., 2008b, Comparing annual MODIS and PRODES forest cover change data for advancing monitoring of Brazilian forest cover. *Remote Sensing of Environment*, **112**, pp. 3783–3793.

HIRSCH, A.I., LITTLE, W.S., HOUGHTON, R.A., SCOTT, N.A. and WHITE, J.D., 2004, The net carbon flux due to deforestation and forest re-growth in the Brazilian Amazon: analysis using a process-based model. *Global Change Biology*, **10**, pp. 908–924.

INPE, 2008, *PRODES Project: Satellite Monitoring of the Brazilian Amazon Forest*. Instituto Nacional de Pesquisas Espaciais. Available online at: www.obt.inpe.br/prodes/ (accessed 10 June 2009).

IVERSON, L.R., COOK, E.A. and GRAHAM, R.L., 1994, Regional forest cover estimation via remote sensing: the calibration center concept. *Landscape Ecology*, **9**, pp. 159–174.

LATIFOVIC, R. and OLTHOF, I., 2004, Accuracy assessment using sub-pixel fraction error matrices of global land cover products derived from satellite data. *Remote Sensing of Environment*, **90**, pp. 153–165.

LATIFOVIC, R., ZHU, Z., CIHLAR, J., GIRI, C. and OLTHOF, I., 2004, Land cover mapping of North and Central America – global land cover 2000. *Remote Sensing of Environment*, **89**, pp. 116–127.

LOWRY, J., RAMSEY, R.D., THOMAS, K., SCHRUPP, D., SAJWAJ, T., KIRBY, J., WALLER, E., SCRADER, S., FALZARANO, S., LANGS, L., MANIS, G., WALACE, C., SCHULZ, K., COMER, P., POHS, K., RIETH, W., VELASQUEZ, S., WOLK, B., KEPNER, W., BOYKIN, K., O'BRIEN, L., BRADFORD, D., THOMPSON, B. and PRIOR-MAGEE, J., 2007, Mapping moderate-scale land-cover over very large geographic areas within a collaborative framework: a case study of the Southwest Regional Gap Analysis Project (SWReGAP). *Remote Sensing of Environment*, **108**, pp. 59–73.

LU, D., BATISTELLA, M., MORAN, E. and DE MIRANDA, E.E., 2008, A comparative study of Landsat TM and SPOT HRG images for vegetation classification in the Brazilian Amazon. *Photogrammetric Engineering and Remote Sensing*, **70**, pp. 311–321.

LU, D., MAUSEL, P., BATISTELLA, M. and MORAN, E., 2004, Comparison of land-cover classification methods in the Brazilian Amazon basin. *Photogrammetric Engineering and Remote Sensing*, **70**, pp. 723–731.

LU, D., MAUSEL, P., BRONDÍZIO, E.S. and MORAN, E., 2002, Assessment of atmospheric correction methods for Landsat TM data applicable to Amazon basin LBA research. *International Journal of Remote Sensing*, **23**, pp. 2651–2671.

LU, D., MORAN, E. and BATISTELLA, M., 2003, Linear mixture model applied to Amazonian vegetation classification. *Remote Sensing of Environment*, **87**, pp. 456–469.

LU, D. and WENG, Q., 2007, A survey of image classification methods and techniques for improving classification performance. *International Journal of Remote Sensing*, **28**, pp. 823–870.

MAYAUX, P. and LAMBIN, E.F., 1995, Estimation of tropical forest area from coarse spatial resolution data: a two-step correction function for proportional errors due to spatial aggregation. *Remote Sensing of Environment*, **53**, pp. 1–15.

MCIVER, D.K. and FRIEDL, M.A., 2001, Estimating pixel-scale land cover classification confidence using nonparametric machine learning methods. *IEEE Transactions on Geoscience and Remote Sensing*, **39**, pp. 1959–1968.

MUSTARD, J.F. and SUNSHINE, J.M., 1999, Spectral analysis for earth science: investigations using remote sensing data. In *Remote Sensing for the Earth Sciences: Manual of Remote Sensing*, 3rd edn, vol. 3, A.N. Rencz (Ed.), pp. 251–307 (New York, NY: John Wiley and Sons).

OLTHOF, I. and FRASER, R.H., 2007, Mapping northern land cover fractions using Landsat ETM+. *Remote Sensing of Environment*, **107**, pp. 496–509.

POTAPOV, P., HANSEN, M.C., STEHMAN, S.V., LOVELAND, T.R. and PITTMAN, K., 2008, Combining MODIS and Landsat imagery to estimate and map boreal forest cover loss. *Remote Sensing of the Environment*, **112**, pp. 3708–3719.

ROBERTS, D.A., BATISTA, G.T., PEREIRA, J.L.G., WALLER, E.K. and NELSON, B.W., 1998, Change identification using multitemporal spectral mixture analysis: applications in eastern Amazônia. In *Remote Sensing Change Detection: Environmental Monitoring Methods and Applications*, R.S. Lunetta and C.D. Elvidge (Eds.), pp. 137–161 (Ann Arbor, MI: Ann Arbor Press).

ROBERTS, D.A., NUMATA, I., HOLMES, K., BATISTA, G., KRUG, T., MONTEIRO, A., POWELL, B. and CHADWICK, O.A., 2002, Large area mapping of land-cover change in Rondônia using decision tree classifiers. *Journal of Geophysical Research*, **107**, 8073, doi:10.1029/2001JD000374.

SABOL, D.E., JR., GILLESPIE, A.R., ADAMS, J.B., SMITH, M.O. and TUCKER, C.J., 2002, Structural stage in Pacific Northwest forests estimated using simple mixing models of multispectral images. *Remote Sensing of Environment*, **80**, pp. 1–16.

SCHWARZ, M. and ZIMMERMANN, N.E., 2005, A new GLM-based method for mapping tree cover continuous fields using regional MODIS reflectance data. *Remote Sensing of Environment*, **95**, pp. 428–443.

SEDANO, F., GONG, P. and FERRAO, M., 2005, Land cover assessment with MODIS imagery in southern African Miombo ecosystems. *Remote Sensing of Environment*, **98**, pp. 429–441.

SHIMABUKURO, Y.E., BATISTA, G.T., MELLO, E.M.K., MOREIRA, J.C. and DUARTE, V., 1998, Using shade fraction image segmentation to evaluate deforestation in Landsat thematic mapper images of the Amazon region. *International Journal of Remote Sensing*, **19**, pp. 535–541.

SHIMABUKURO, Y.E. and SMITH, J.A., 1991, The least-squares mixing models to generate fraction images derived from remote sensing multispectral data. *IEEE Transactions on Geoscience and Remote Sensing*, **29**, pp. 16–20.

SHIMABUKURO, Y.E. and SMITH, J.A., 1995, Fraction images derived from Landsat TM and MSS data for monitoring reforested areas. *Canadian Journal of Remote Sensing*, **21**, pp. 67–74.

SIVANPILLAI, R., SRINIVASAN, R., SMITH, C.T., MESSINA, M.G. and WU, X.B., 2007, Estimating regional forest cover in East Texas using Advanced Very High Resolution Radiometer (AVHRR) data. *International Journal of Applied Earth Observation and Geoinformation*, **9**, pp. 41–49.

SKOLE, D.L., CHOMENTOWSKI, W.H., SALAS, W.A. and NOBRE, A.D., 1994, Physical and human dimension of deforestation in Amazonia. *BioScience*, **44**, pp. 314–328.

SMITH, M.O., USTIN, S.L., ADAMS, J.B. and GILLESPIE, A.R., 1990, Vegetation in deserts: a regional measure of abundance from multispectral images. *Remote Sensing of Environment*, **31**, pp. 1–26.

THESEIRA, M.A., THOMAS, G., TAYLOR, J.C., GEMMELL, F. and VARJO, J., 2003, Sensitivity of mixture modeling to endmember selection. *International Journal of Remote Sensing*, **24**, pp. 1559–1575.

TIAN, H., MELILLO, J.M., KICKLIGHTER, D.W., McGUIRE, A.D., HELFRICH, J., MOORE, III, B. and VÖRÖSMARTY, C.J., 1998, Effect of interannual climate variability on carbon storage in Amazonian ecosystems. *Nature*, **396**, pp. 664–667.

TOTTRUP, C., RASMUSSEN, M.S., EKLUNDH, L. and JONSSON, P., 2007, Mapping fractional forest cover across the highlands of mainland Southeast Asia using MODIS data and regression tree modeling. *International Journal of Remote Sensing*, **28**, pp. 23–46.

VAN DER MEER, F. and DE JONG, S.M., 2000, Improving the results of spectral unmixing of Landsat thematic mapper imagery by enhancing the orthogonality of end-members. *International Journal of Remote Sensing*, **21**, pp. 2781–2797.

VIEIRA, I.C.G., DE ALMEIDA, A.S., DAVIDSON, E.A., STONE, T.A., DE CARVALHO, C.J.R. and GUERRERO, J.B., 2003, Classifying successional forests using Landsat spectral properties and ecological characteristics in eastern Amazonia. *Remote Sensing of Environment*, **87**, pp. 470–481.

WANG, Q. and TENHUNEN, J.D., 2004, Vegetation mapping with multitemporal NDVI in North Eastern China Transect (NECT). *International Journal of Applied Earth Observation and Geoinformation*, **6**, pp. 17–31.

WASER, L.T. and SCHWARZ, M., 2006, Comparison of large-area land cover products with national forest inventories and CORINE land cover in the European Alps. *International Journal of Applied Earth Observation and Geoinformation*, **8**, pp. 196–207.

WESSELS, K.J., DeFRIES, R.S., DEMPEWOLF, J., ANDERSON, L.O., HANSEN, A.J., POWELL, S.L. and MORAN, E.F., 2004, Mapping regional land cover with MODIS data for biological conservation: examples from the Greater Yellowstone Ecosystem, USA and Pará State, Brazil. *Remote Sensing of Environment*, **92**, pp. 67–83.

ZHU, Z. and EVANS, D.L., 1994, US forest types and predicted percent forest cover from AVHRR data. *Photogrammetric Engineering and Remote Sensing*, **60**, pp. 525–532.